# Prosthetic Arm Using EEG Control Signals Based on Deep Convolutional Neural Network

Amr Mostafa*, Fady Mostafa, and Sara Ahmed
*Helwan university, Egypt, Eng.Amr.omar99@gmail.com , Eng.FadyOmar@gmail.com, sarahelbokhari@gmail.com*

*Supervisor:* Taha H. S. Abdelaziz, Dr
*Helwan university, Egypt, taha_ abdelaziz@h-eng.helwan.edu.eg*

*Supervisor:* Marwa M. A. Hadhoud, Dr
*Helwan University, Egypt, marwa_hadhoud@h-eng.helwan.edu.eg*

*Supervisor:* Ibrahim Sadek, Dr
*Helwan University, Egypt, ibrahim_ibrahim@h-eng.helwan.edu.eg*

***Abstract– Huge number of people Suffer from amputations or neurological damages, which prevent them from interacting with their environment in a simple and normal way. According to WHO report in 2021, there are more than 30-million amputee patient all over the world and the main percentage of them are arm amputees. Most prosthetics arm that uses Brain computer interface technique (BCI) are only work in lab scale. Some of them is invasive and require dangerous medical surgery to implant electrodes in the gray matter beneath scalp or use noninvasive sensor but need huge number of electrodes to compensate the loss of EEG signals. We worked on dataset include 32 EEG electrodes according to 10-20 standardization and select only 6 electrodes that are relevant to arm movement. Our proposed system includes three main stages, preprocessing of EEG signal through making band bass, CSP filters and apply CWT. In the second stage, we trained data on pretrained network -VGG16- for feature extraction. Finally, we implement our classification model on the robotic arm. We depend on accuracy and loss to evaluate classification model and built GUI by LabVIEW to determine kinematics and dynamics calculation for robotic arm. We managed to control robotic arm that closely mimics the human arm based on EEG signal and the performance of our proposed classification algorithm is evaluated in terms of accuracy with average 90.2% which can help amputees to perform their daily lives as normal people without the need for assistance from others.***

***Keywords-- Brain computer interface; CSP; Prosthetic.***

## I. INTRODUCTION

Brain computer interface was just an idea or a dream to combine human brain with computer systems years ago. It has been a point of study from scientists and researchers in how to capture signals from human brain to control external electronic devices. Currently, researchers managed to achieve this dream in real ground thanks to science of brain computer interface. It is expected BCI will offer promising solutions in the coming few years for people who have physical impairments. Human brain is complicated as it has about 100 billion neurons for that, we can consider it as a general-purpose computer. It consists of two main parts; first is sub-cortical region, which responsible for some essential functions such as respiration, body temperature, heart rate, learning, memory, and emotional response. Second part is cerebral cortex, which is the most complicated region in the human brain as it consists of two hemispheres. Each hemisphere divided into four lobes: parietal, frontal temporal, and occipital. The vital functions of cerebral cortex include planning, language processing and pattern recognition thus, it will be the point of study from BCI researchers. Brain computer interfaces (BCIs) based on electroencephalograms (EEGs), are one of the most clinically studied BCI technologies due to being a non-invasive technique, and having good temporal resolution, ease of use, portability, and a low set-up cost. Significant research is being done to treat individuals with neurological impairment brought on by an accident through using EEG-based BCI. The main concept is to have a control algorithm that processes EEG signals based on the user's intent. However, the highly non-stationary and large intersession variation of EEG signals poses a significant challenge in the development of EEG-based BCI. EEG signals can be distinguished in general by their amplitude, frequency, and electrode position. Because signals in this band are associated with senses such as touch, hearing, smell, and taste, waves are most likely associated with actions and behavior. Waves in the frequency range of (13 Hz to 30 Hz) occur in a conscious state, whereas waves in the frequency range of (8 Hz to 13 Hz) are associated with motor cortex functions. These waveforms are obtained from electrodes located throughout the motor cortex, specifically the C3, Cz, and C4 locations, which control body sensory and motor functions. Furthermore, because they are associated with cognitive processing in the brain, parietal electrodes such as P3, Pz, and P4 can be used to classify the motor movement signal. Raw EEG recordings may contain artefacts from both external and internal sources. The 60 Hz power line frequency component

is the primary source of external artefacts, whereas internal artefacts are caused by bioelectric potentials from eye blinking or muscle potentials caused by jaw and facial movements. According to Singhal et al., the specific frequency associated with artefact signals such as eye blinking is less than 4 Hz, artefacts from heartbeats are around 1.2 Hz, and muscle artefacts are more than 30 Hz. Using a band pass filter to remove unwanted frequencies while retaining the frequency band of interest is one method for removing these artefacts. Furthermore, the EEG signal has drawbacks such as a low signal-to-noise ratio and a low spatial resolution. As a result, researchers are constantly looking for improved methods to extract features of synchronization and desynchronization events during motor imagery, such as using the common spatial pattern (CSP) method. Furthermore, frequency domain analysis of a 1D signal can be efficient, particularly for noise-sensitive EEG signals. Wavelet transform converts 1D time domain signals to 2D frequency domain signals and can be analyzed at multiple resolutions. Scalogram is the name given to the 2D frequency domain signal.

### *A. Related Studies*

The decoding of hand movements from EEG signals for assistive technology applications such as controlling a prosthetic device has been studied over the last decade. Li et al., used connectivity analysis based on EEG as the feature for decoding voluntary right-hand movement in their research on decoding the movement of wrists, upper limbs, elbows, and shoulders. The most sensitive EEG components have been found to be the gamma, delta, and theta bands of electrodes in the premotor and somatosensory motor cortex. In recent years, many papers on the classification of motor imagery EEG signals using CSP have been published. Wang et al. proposed in for imagery hand and foot movement classification the selection of channels based on maximum spatial pattern vectors in scalp mapping, readiness potential and combined with event-related desynchronization. For multiclass classification of motor imagery EEG signals, methods that combine both filter bank and CSP are used. Prior to use CSP technique for feature extraction, EEG data is separated into many frequency bands using a filter bank, which improved motor imagery task classification accuracy. The proposed sub band regularized CSP for motor imagery EEG classification used a filter bank that splits EEG signals in the 4-40 Hz range into 4 Hz wide sub bands. The proposed method produced classification accuracy ranging from 63.78% to 98.21% for five subjects. Robinson investigated the use of CSP for real-world motor EEG signals. The goal was to decode data and information from human brain that collected through hand movement experiment.

In this study, we propose a new method for feature extraction and classification of grasp and lift EEG data using a pre-trained network (VGG16). We choose six specific electrodes that have a high influence on motor signals (C3,C4,Cz,P3,P4,Pz), and then apply band pass filter to remove noise before normalizing them through using mean value and standard deviation. Following that, the signal is fed through a CSP filter to improve signal discrimination between classes before being converted to frequency domain using the CWT to produce scalogram images. The scalogram images are then sent to a pre-trained network to classify dataset movements. Finally, we interfaced the decision of pretrained network with prosthetic arm to perform specific tasks through GUI designed by LabVIEW. The flow of this paper is organized in the following sequence. Section 2 covers materials and methods used in our proposed system. Section 3, illustrate and discuss experimental results of paper. Section 4 concludes the paper and suggests further work.

## II. MATERIAL AND METHODS

### *A. Processing EEG Signals*

#### *1) Dataset*

The grasp-and-lift EEG dataset was sponsored by the wearable interfaces for hand function recovery consortium with the target of understanding the relationship between human movement, EEG signals, and BCI devices to help patients with neurological disabilities. Data was collected using an EEG recording device known as AntiCap, which has 32 electrodes and a sampling frequency of 500 Hz. The dataset is made up of EEG recordings of grasp-and-lift tasks collected from 12 healthy subjects. Each subject performed 10 series of trials, with approximately 30 trials in each series. The location of the electrode was determined using the 10 to 20 system positioning. During data collection, each subject was instructed to reach for an object, lift it with their thumbs, hold it in the air, and then place it in various positions. The dataset's event label is captured using data from four 3D position sensors that record the position and orientation of the object, the index finger, the thumb, and the wrist. The position is recorded in Cartesian coordinates x, y, and z, and the orientation is recorded in azimuth, elevation, and roll. Two surface contact plates on the object's sides were each connected to a force transducer that recorded three force and three torque channels. Many events were identified using a combination of first- and second-time derivatives of the relevant signals. Before computing these derivatives, all signals were smoothed with Savitzky-Golay filtering to increase the precision of the data without distorting the signal.

#### *2) Channel Selection*

The EEG channels chosen for the grasp-and-lift tasks will carry the majority of the information related to motor function. Based on the movement correlation for the grasp-and-lift tasks, six out of 32 channels are chosen: C4, C3, Cz, P4, P3, and Pz. P4, P3, and Pz are associated with cognitive processing in the brain , whereas C4, C3, and Cz are related to motor movement.

#### *3) Filter and Normalization*

The EEG data is band pass filtered with cut-off frequencies in between 7 and 30 Hz to easily extract EEG signals in the μ and β bands. The use of this band eliminates artefacts (around 1.2 Hz) related to heartbeat , while (below 4 Hz) associated with eye blink, and muscle movement (above 30 Hz) in EEG signals because these artefacts are essentially

outside the μ and β band and after that we apply CSP filtering technique to improve performance of neural network in classifying different events of data. Normalizing band pass filtered EEG data involves subtracting the mean and dividing by the signal's standard deviation.

4) Continuous Wavelet Transformation

Continuous wavelets transform (CWT) is a popular method for converting 1D signals into a 2D frequency domain matrix. As a time-frequency transform, the wavelet transform is known to be more powerful than the conventional cosine and Fourier transforms. In contrast to the Fourier transform, which generates spectrograms with fixed time and frequency resolution, the wavelet transform incorporates multiple scales and thus provides optimal time-frequency resolution. A 2D matrix known as a scalogram will generate when we apply wavelet transforms of CSP filtered EEG signals, which is the absolute value of a signal's CWT coefficients, and we use the analytic Morlet as a wavelet filter bank. The wavelet maximum and minimum scales are calculated automatically based on the wavelet's energy spread in time and frequency domain. Because the scalogram images of the wavelet transform are 69×400, they must first be resized to 224×224 using bicubic interpolation. This step is required because the pretrained VGG16 will only accept input with an image size of 224×224 pixels.

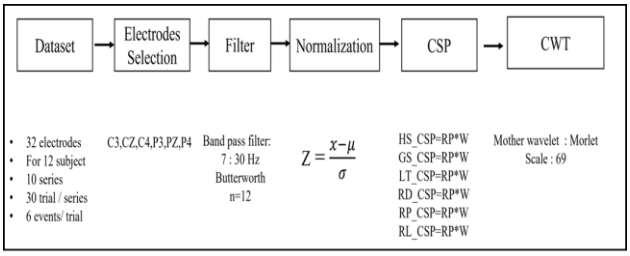


Fig. 1 Proposed Processing Stages of EEG signals .

## B. *Pre-Trained Network*

A pre-trained model is one that has already been trained on a huge dataset and contains biases and weights that represent the features of the dataset on which it was trained. Learned characteristics are frequently transferable to new data. A model trained on a dataset ,it contains learned features such as horizontal lines or edges which are transferable to any dataset and can save time and benefit from previous learned features. VGG16 is considered as CNN model proposed by A. Zisserman and K. Simonyan from Oxford University. This network achieves 92.7% top-5 test accuracy on ImageNet dataset which contain over 14 million images classified into 1000 classes. The input layer of Vgg16 is RGB image in size 224×224. The image is moved through a convolutional layer, with the filters set to capture the notions of left/right, up/down, and center with a very small receptive field: 33 (the smallest size to capture the notions of left/right, up/down, and center). It also employs 11 convolution filters in one of the configurations, which can be thought of as a linear transformation of the input channels (followed by non-linearity). The convolution stride is set to 1 pixel, and the spatial padding of conv. All hidden layers include the rectification (ReLU) non-linearity as activation function.

## C. *Mechatronic System*

The main goal of our mechatronic system is to obtain neural network output and then translate it into commands that actuators can use to perform desired tasks. So, in this section, we will go over the main components of our system.

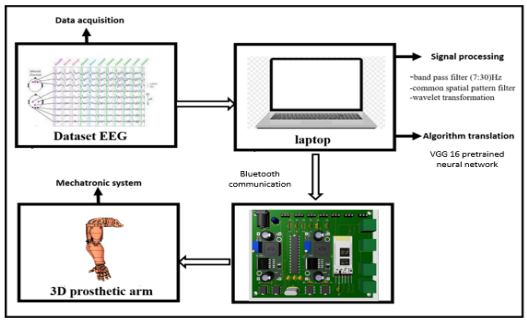


Fig. 2 Main stages of Mechatronic System.

1) Mechanical Aspects

Our prosthetic Arm was consisting of 2 degree of freedom planer robot arm designed to mimic human arm. It was built from lightweight material (PLA) using 3D printing technology. The full length of Prosthetic arm is around 80 cm with total weight 2.25 Kg. It includes four main parts which are hand, forearm, Biceps, and shoulder. It can perform several tasked such as hand-checking, reach and grasp items which allowing arm to have realistic and sophisticated behavior.

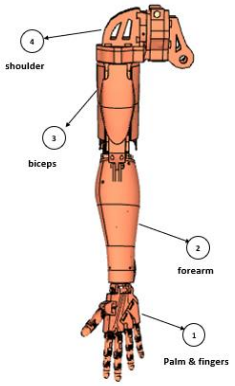


Fig. 3 Elements of electromechanical prosthetic arm.

2) Kinematics

Kinematics describes the motion of mechanical systems, it also deals with velocities and accelerations, which are defined for points of interest on the mechanical systems. The description of motion is relative in nature. Velocities and accelerations are therefore defined with respect to a reference frame.

2.1) Forward Kinematics

The Forward Kinematics concerned with the relationship between the individual joints of the robot manipulator and the tool or end-effector position and orientation. The target of forward kinematics is to determine the position and orientation of the end effector through the given values for the robot's joint variables. In the case of revolute or rotational joints, the joint variables are the angles between the links.

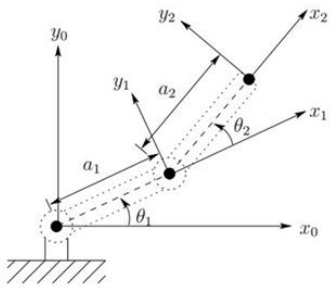


Fig. 4 Prosthetic arm free body diagram .

We apply D-H parameter to deduce transformation matrix as the following equations:

| Joint # I | Joint type | $\theta_i$ | $\alpha_i$ | $d_i$ | $a_i$ |
|---|---|---|---|---|---|
| 1 | Revolute | $\theta_1(t)$ | 0 | 0 | $l_1$ |
| 2 | Revolute | $\theta_2(t)$ | 0 | 0 | $l_2$ |

Table. 1 D-H parameters of prosthetic arm.

$$^0T_2 = {}^0T_1\ {}^1T_2$$

$$^0T_2 = \begin{bmatrix} Cos\,\theta1 & -Sin\,\theta1 & 0 & L_1Cos\,\theta1 \\ Sin\,\theta1 & Cos\,\theta1 & 0 & L_1Sin\,\theta1 \\ 0 & 0 & 1 & 0 \\ 0 & 0 & 0 & 1 \end{bmatrix} \begin{bmatrix} Cos\,\theta2 & -Sin\,\theta2 & 0 & L_2Cos\,\theta2 \\ Sin\,\theta2 & Cos\,\theta2 & 0 & L_2Sin\,\theta2 \\ 0 & 0 & 1 & 0 \\ 0 & 0 & 0 & 1 \end{bmatrix}$$

$$^0T_2 = \begin{bmatrix} Cos\,\theta1\,Cos\,\theta2 & -Sin\,\theta1\,Sin\,\theta2 & 0 & L_1Cos\,\theta1 + L_2Cos\,\theta2 \\ Sin\,\theta1\,Sin\,\theta2 & Cos\,\theta1\,Cos\,\theta2 & 0 & L_1Sin\,\theta1 + L_2Sin\,\theta2 \\ 0 & 0 & 1 & 0 \\ 0 & 0 & 0 & 1 \end{bmatrix}$$

3) Dynamics

It is concerned with the relationship between the forces acting on a robot mechanism and the accelerations produced as a result of those forces. Robot dynamics is the application of rigid-body dynamics to robots when the robot mechanism is typically modelled as a rigid-body system. Forward dynamics is also known as direct dynamics or dynamics in some cases. Inverse dynamics has a variety of applications, including on-line control of robot motions and forces, trajectory design and optimization, robot mechanism design, and as a component in some forward dynamic's algorithms. Torques calculation of our proposed prosthetic arm is determined by lagrangian equations as the following:

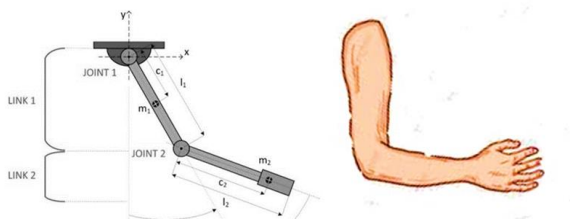


Fig. 5 Dynamic analysis for prosthetic arm.

For link1, the force component $\tau_1$ is determined in the final form :

$$\tau_1 = \left[m_1.c_1^2 + m_2.c_2^2 + m_2.l_1^2 + 2m_2.c_2^2.l_1.cos\,\theta_2 + I_1 + I_2\right].\ddot{\theta_1} + \left[m_2.c_2^2 + m_2.c_2.l_1.cos\,\theta_2 + I_2\right].\ddot{\theta_2} - 2m_2.c_2.l_1.sin\,\theta_2.\dot{\theta_1}.\dot{\theta_2} - m_2.c_2.l_1.sin\,\theta_2.\dot{\theta_2}^2 + m_2.g.c_2.sin(\theta_1 + \theta_2) + \left[m_1.c_1 + m_2.l_1\right].g.sin\,\theta_1$$

For link2, the force component $\tau_2$ is determined in the final form :

$$\tau_2 = \left[m_2.c_2^2 + m_2.c_2.l_1.cos\,\theta + I_2\right].\ddot{\theta_1} + \left[m_2.c_2^2 + I_2\right].\ddot{\theta_2} + m_2.c_2.l_1.sin\,\theta_2.\dot{\theta_1}^2 + m_2.g.c_2.sin(\theta_1 + \theta_2)$$

4) Hardware Overview

4.1) Atmega328p

We use the Atmega328p because it is one of the most popular microcontrollers due to its features and low cost. It contains 28 pins and many of them have more than one function. It can work on embedded systems and executes programs quickly due to its advanced RISC architecture.

4.2) Power supply

we first determine the maximum voltage and current in the circuit thus , 12 volts is the maximum voltage and the maximum current available is 3 amps. However, we will not use all motors at the same time for an extended period. We will take 12 volts from power supply and use a DC-DC buck converter to reduce the voltage to 5 volts for our proposed control circuit.

4.3) Servo motor

A servo motor is a type of motor that can rotate with great precision. Normally this type of motor consists of a control circuit that provides feedback on the current position of the motor shaft, this feedback allows the servo motors to rotate with great precision. We used the following servo motor in our prosthetic arm, (Mg995R) for each finger, (Mg996R) for biceps flexion and extension and finally, (FS5113R) for shoulder forward and backward movements.

4.4) HC-05 Bluetooth Module

The HC-05 Bluetooth module is intended for wireless communication. This module can be used as either a master or a slave. Bluetooth serial modules enable all serial-enabled devices to communicate wirelessly with one another .We used this module to receive output of neural network from LabVIEW and send it to microcontroller for performing desired movements by prosthetic arm.

Fig. 6 Pcb electronic circuit design .

## III. Result and Discussion

This section begins with a summary of the grasp-and-lift EEG recordings, band pass filtered data, and CSP filtered data. Results on the classification of six-class motor events by our proposed methodology ( CSP, CWT, and pre-trained Vgg16) were then investigated and appeared satisfied results .Training and testing of Vgg16 was implemented on the Python platform and ran on a Colab. The calculation of position, velocity , acceleration, and torque for each joint are implemented and graphed by GUI designed through LabView.

### *A) Bandpass filter and normalize.*

The raw and band pass filtered EEG data contain the six grasp-and-lift events for subject 1 in dataset. The band pass filtered signal will be in range 7 and to 30 Hz, through eliminating artefacts such as power line noise, eye blinking, , muscle artefacts and heartbeat artefacts. The lower stopband frequency of a finite impulse response filter is set at 5 Hz, while the upper stopband frequency is set at 33 Hz. The stopband attenuation is set to 65 dB . The graph below depicts 2400 samples of six events from the P3 channel before and after filtering and normalization.

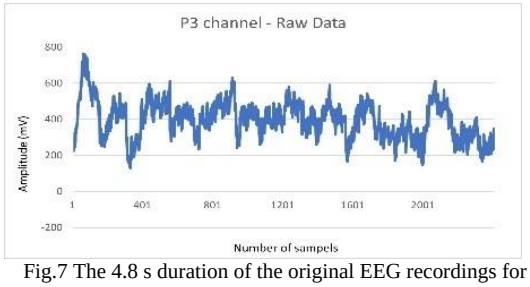


Fig.7 The 4.8 s duration of the original EEG recordings for subject 1 from electrode P3, comprising the six grasp-and-lift motor events, HS, GS, LT, HD, RP and RL

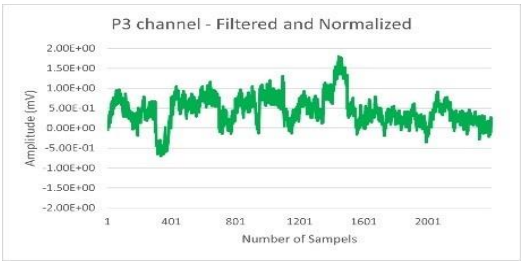


Fig.8 The 4.8 s duration of the band pass filtered and normalized EEG recordings for subject 1 from electrode P3, comprising the six grasp-and-lift motor events, HS, GS, LT, HD, RP, and RL

### *B) Common Spatial Pattern (CSP) Filtering*

As discussed in section 2, w produces the greatest variance in one class and the smallest variance in the other in data transformed by CSP filtering. Figures 10 and 11 show a 3D scatter plot of the (C4, Cz, C3) electrodes and (P4, Pz, P3) electrodes generated for GS vs. NonGS events. Remarkably, GS values are dispersed across a larger 3D space prior to CSP filtering, but the values are mapped to a much smaller 3D space after CSP filtering. The other five events follow the same pattern. The concept of maximal oriented energy is a key feature of CSP that contributes to its success in two-class event classification.


Fig.9 CSP filtering is based on a matrix decomposition method.

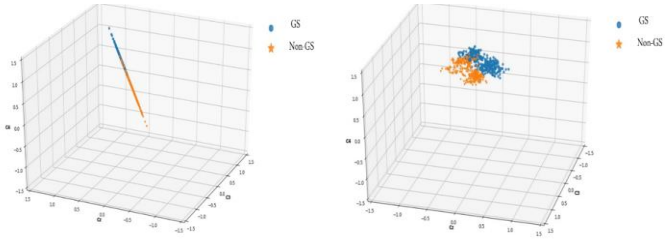


Fig.10 The 3D-scatter plots of 300 samples of EEG for HS vs. Non-HS events from (C3, Cz, C4) electrodes are plotted after and before CSP filtering.

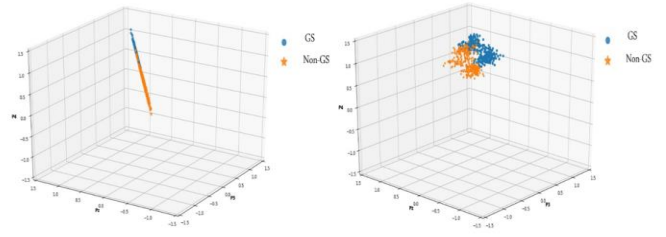


Fig.11 The 3D-scatter plots of 300 samples of EEG for HS vs. Non-HS events from (P3, Pz, P4) electrodes are plotted after and before CSP filtering.

### C) Classification Events using CSP, CWT and Vgg16

In this experiment, we use Vgg16 to assess the performance of the CSP-CWT algorithm in classifying EEG grasp-and-lift motor functions. Vgg16, a deep learning network capable of capturing both high-level and low-level spatial features of scalograms, plays the role of feature extraction and classifier in this case. The size of the sliding window used for wavelet scalogram conversion is 400 samples, which is equal to 0.8 second duration with overlap 100 samples. Each electrode will generate a grayscale scalogram. Three grayscale scalograms of size 224×224×1 from the same group's electrodes C4, Cz, and C3 are concatenated to form an RGB scalogram of size 224×224×3. Electrode P4, Pz, and P3 will produce similar RGB scalograms. There are 6960 scalograms that equally generated in total from all classes (HS, GS, LT, HD, RP, and RL).

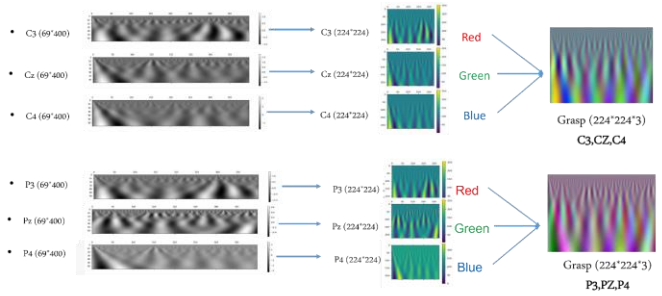


Fig.12 Formation of scalogram images of EEG motor function from electrode C3, Cz, C4, P3, Pz and P4 using CWT.

The RGB scalogram images are divided training and testing into with a ratio of 0.8:0.2. We use Vgg16 to train the model for classifying the six classes. Validating data is used to validate accuracy at each epoch to reduce overfitting, while testing data is used to test accuracy after training. The training option's maximum epochs are set to 40. The accuracy for classification six motor events of dataset by our proposed methodology CSP-CWT, tested in the framework of one-versus-all.

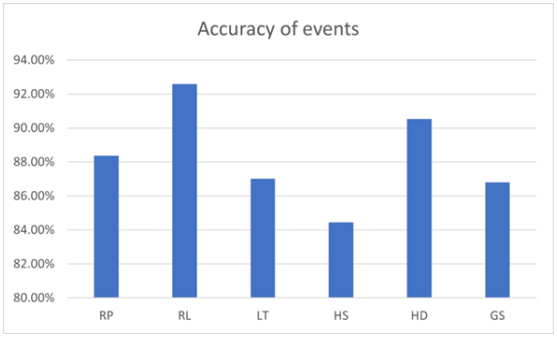


Fig.13 Accuracy for all 6 events of dataset

### D) Robotic Arm Analysis

We use LabView to make simulation for our proposed prosthetic arm and check each of position, velocity , acceleration, and torque for each joint for LT movement. Then, we applied kinematics parameters of our prosthetic arm, and dynamic parameters of each link which include, mass, center of gravity, gear ratio and inertia matrix of each link which we have previously explained in section 2. Results of this semi real time scenario study were satisfied and showed the efficiency of our proposed prosthetic arm .

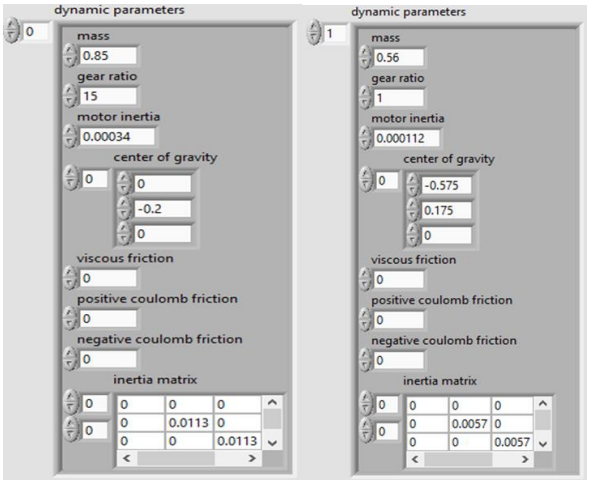


Fig.14 Dynamic parameters

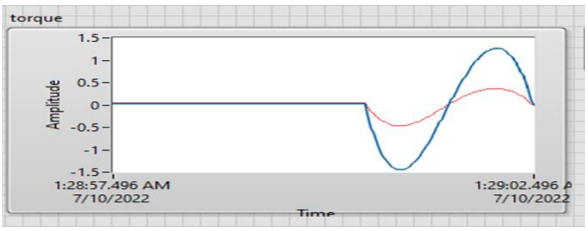


Fig.15 Torque Trajectory

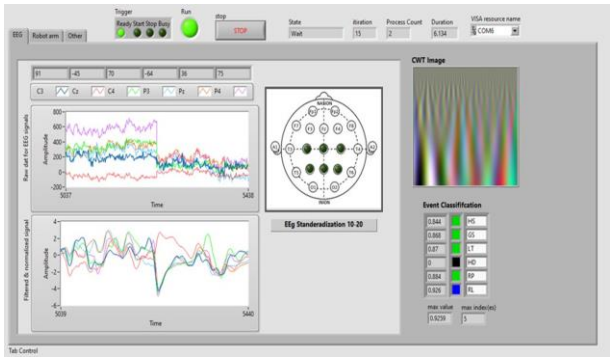


Fig.16 LabView GUI for signal processing

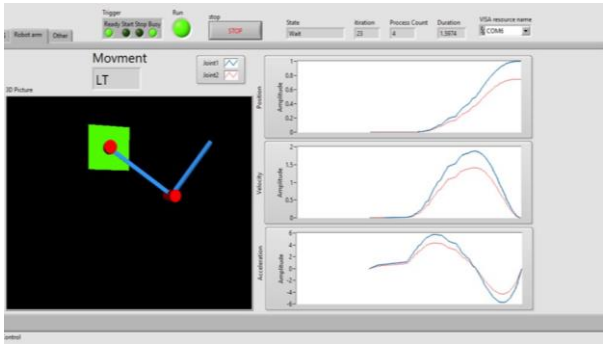


Fig.17 LabView GUI calculation for each joint in term of position, velocity, and acceleration.

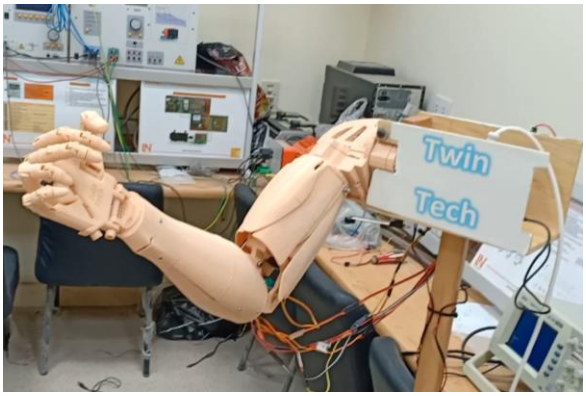


Fig.18 Fingers and biceps extension while receiving EEG signals from LabView.

## IV. Conclusion and Future Work

In this study, we presented a brain-controlled prosthetic arm based on CSP, CWT and -Vgg16- deep convolutional neural network. We depend on accuracy and loss to evaluate classification model and built GUI by LabVIEW to visualize signal processing of dataset and determine calculations of kinematics and dynamics for robotic arm. Our proposed prosthetic arm is similar to the humanoid arm as it consists of 2-links and an end effector as much close to the natural arm. It also can perform several tasks such as hand reaching, grasping items, making extensions, and flexion for each finger independently. We evaluated our proposed semi real time system in terms of accuracy with average 90.2% which can help amputees to perform their daily lives as normal people without the need for assistance from others.

**Furthermore**, we will implement our model on a real BCI scenario through using open BCI kit and reduce number of electrodes to just only 3 electrodes. On the other hand , we will increase number of DOF (degree of freedom) to 7 that can enable us to mimic natural human arm and perform more tasks.

## Acknowledgment

We would like to thank Eng. Ibrahim Badawy from mechatronics engineering department at Helwan university for his support during our graduation project. Also, we would like to thank and appreciate our beloved parents who have stood by us and afforded the total cost of this study.

## References

[1] Yahya, Norashikin & Musa, Huwaida & Ong, Zhong & Elamvazuthi, Irraivan. (2019). Classification of Motor Functions from Electroencephalogram (EEG) Signals Based on an Integrated Method Comprised of Common Spatial Pattern and Wavelet Transform Framework. Sensors. 19. 4878. 10.3390/s19224878.

[2] N. Birbaumer, W. Heetderks, J. Wolpaw, W. Heetderks, D. McFarland, P. H. Peckham, G. Schalk, E. Donchin, L. Quatrano, C. Robinson and T. Vaughan, “Brain-Computer Interface Technology: A Review of the First International Meeting,” IEEE Transaction on Rehabilitation Engineering,vol. 8, no. 2, pp. 164-173, 2000.

[3] F. Lotte, L. Bougrain, M. Clerc, F. Lotte, L. Bougrain, M. Clerc, E. Eeg, F. Lotte, L. Bougrain, and M. Clerc, Interfaces To cite this version: Electroencephalography (EEG) -based Brain-Computer Interfaces. 2015.

[4] Johan J.Craig, Introduction to Robotics Mechanics and Control, 3rd Edition, pp 109-114, Prentice Hall, 2005. Abledata, [Online]. Available: ⟨http://www.abledata.com⟩ .

[5] Wittenburg, J. (2016). Kinematics: Theory and Applications (1st ed. 2016 ed.). Springer.

[6] H. Nakasaki, T. Mitomi, T. Noto, K. Ogoshi, H. Hanaue, Y. Tanaka, H. Makuuchi, H. Clausen, S.I. Hakomori, Mosaicism in the expression of tumor-associated carbohydrate antigens in human colonic and gastric cancers, Cancer Res. 49 (13) (1989) 3662–3669.

[7] D. Tan, A. Nijholt, Brain-Computer Interfaces, (Human-Computer Interaction Series), in: Desney S. Tan, Anton Nijholt (Eds.), Brain-Computer Interfaces_ Applying our Minds to Human-Computer Interaction, Springer-Verlag L., 2010.

[8] Mostafa, Amr & Mostafa, Fady. (2021). Brain Computer Interface: A Scoping Review.